

Figure 6. Depiction of ion-molecule recombination by  $l \rightarrow j$  angular momentum transfer.

for a fixed  $E_{rel}$ . For collisions which occur with small values of  $b$ , the dominant energy-transfer mechanism leading to recombination is expected to be  $T \rightarrow V$ . As the value of  $b$  for the collision approaches  $b_m$ , the  $T \rightarrow R$  process is expected to compete with  $T \rightarrow V$  as a result of the collisional orbital angular momentum. The insensitivity of  $P(E_{rel}, b)$  to  $b$  for  $b < b_m$  and  $E_{rel}$  a constant indicates that these two energy-transfer processes have similar efficiencies for ion-molecule recombination.

## VII. Conclusion

This quasiclassical trajectory study has shown that there are interesting and important dynamical features involved in ion-molecule recombination reactions. Formation of the ion-molecule

collision complex requires that the initial relative translational energy be transferred to rotational and/or vibrational degrees of freedom. In order to understand this energy-transfer process, the structure and internal degrees of freedom for both the ion and molecule must be considered.

Only electrostatic intermolecular potentials have been considered in this work. However, the results may have important ramifications for ion-molecule reactions in which chemical bond ruptures and formations take place. In such reactions there are often two important minima on the potential energy surface.<sup>1-3</sup> One results from the long-range electrostatic interactions. The other is formed by the stronger short-range chemical interactions. It is usually assumed that the ion-molecule complex is first trapped in the long-range minimum, and, after intramolecular energy transfer into the proper internal coordinates occurs, the complex moves into the deeper short-range minimum. This study indicates that for some ion-molecule reactions trapping of the complex in the long-range minimum may be an inefficient process. Thus, the long-range intermolecular potential will not determine the rate of the ion-molecule reaction. Such an effect has been seen in several experimental studies.<sup>50-52</sup> Calculating trajectories on potential energy surfaces which have both the short- and long-range minima is an important research topic for future studies.

**Acknowledgment.** This research was supported by the National Science Foundation.

**Registry No.** H<sub>2</sub>O, 7732-18-5; K<sup>+</sup>, 24203-36-9; Na<sup>+</sup>, 17341-25-2; Li<sup>+</sup>, 17341-24-1; (CH<sub>3</sub>)<sub>2</sub>O, 115-10-6.

(50) L. Bass, W. J. Chesnavich, and M. T. Bowers, *J. Am. Chem. Soc.*, **101**, 5493 (1979).

(51) J. J. Grabowski, C. H. DePuy, and V. M. Bierbaum, *J. Am. Chem. Soc.*, **105**, 2565 (1983).

(52) R. R. Squires, V. M. Bierbaum, J. J. Grabowski, and C. H. DePuy, *J. Am. Chem. Soc.*, **105**, 5185 (1983).

## Bound Pyrene Excimer Photophysics and the Organization and Distribution of Reaction Sites on Silica

C. H. Lochmüller,\*† A. S. Colborn,† M. L. Hunnicutt,† and J. M. Harris†

Contribution from the Paul M. Gross Chemical Laboratory, Duke University, Durham, North Carolina 27706, and the Department of Chemistry, University of Utah, Salt Lake City, Utah 84112. Received November 14, 1983

**Abstract:** A study of the time-dependent luminescence of pyrene silane molecules chemically bound to microparticulate silica was undertaken to determine the distribution of molecules chemically bound to silica and their organization in contact with different solvents. The results indicate that the organization and proximity of such molecules are controlled primarily by an inhomogeneous distribution of chemically reactive silanols on the surface. Analysis of the monomer emission decay profiles at several different surface concentrations indicates that the bound molecules are clustered predominantly into regions of high density. Dynamic, solvent-induced conformation changes of the bound molecules were observed in the excimer and monomer emission decay profiles.

A recent article reported on the steady-state luminescence of pyrene silane molecules chemically bound to silica and suggested that clustering of molecules is significant even at less than 10% of the total attainable surface coverage.<sup>1</sup> The resulting picture of the derivatized surface was one of high-density patches of alkyl ligands in contrast to the uniform and relatively ordered blanket that has been envisioned in other reports.<sup>2</sup> An understanding

of the microscopic organization of chemically modified silica surfaces is of particular importance to separation science, especially if one considers the widespread use of such materials as bonded phases in liquid chromatography. Recent studies provide an improved understanding of the influence of solvent modification of the bonded phase on the solute distribution process in re-

\*Duke University.

†University of Utah.

(1) Lochmüller, C. H.; Colborn, A. S.; Hunnicutt, M. L.; Harris, J. M. *Anal. Chem.* **1983**, *55*, 1344.

(2) Unger, K. K.; Roumeliotis, P. *J. Chromatogr.* **1978**, *149*, 211.

versed-phase liquid chromatography and indicate that the extent of solvent penetration into the bonded phase is dependent on the bonded alkyl chain length, surface coverage, and nature of the solvent.<sup>3-7</sup> While structural models have been inferred from such studies, little direct experimental evidence exists on the microscopic structure and organization of the bonded phase.

We report here results obtained by time-dependent luminescence spectroscopic studies of [3-(3-pyrenyl)propyl]dimethylchlorosilane [3PPS] bonded to a microparticulate, macroporous silica gel. The results obtained provide quantitative estimates of the proximity and distribution of chemically accessible silanols on the native silica substrate and the effect of bonded ligand surface concentration and conditioning solvent on the physical organization and distribution of molecules covalently bound to a microparticulate silica. It is believed that these results will contribute to an improved dynamic physicochemical model of the surface structure of *n*-alkyl chemically modified silicas and the underivatized silica substrate, to studies of polymers grafted on surfaces, and to the photophysics of intramolecular excimers.

### Experimental Section

The silica gel used was Whatman Partisil-10 ( $N_2$  surface area of 323  $m^2/g$ , mean pore diameter of 93 Å, and a mean particle diameter of 10  $\mu m$ ). The pyrene silane was synthesized and its structure confirmed in our laboratory. Reagent grade chloroform was dried by distillation from and stored over calcium chloride prior to its use. Spectral grade methanol, acetonitrile, hexane, and tetrahydrofuran were used without further purification, although special precautions were taken to ensure that the tetrahydrofuran did not form peroxides. The silica derivatization procedure and subsequent treatment of the chemically modified silica are detailed in a previous report.<sup>1</sup> The surface concentration of bound silane ( $\mu mol/m^2$ ) was determined by elemental analysis, and the values of the expected average distance between chemically bound pyrene molecules ( $D_{exp}$ ) were calculated by the method of Unger et al.<sup>2</sup>

Time-dependent measurements were made with a Photochemical Research Associates System 2000 nanosecond fluorimeter. All silica samples were subjected to 3 cycles of freeze-pump-thaw to remove oxygen and were packed into a quartz column flow cell described previously.<sup>1</sup> An infusion pump delivered argon-saturated solvents continuously to the flow cell, and no change in count rate was observed during the analysis time. The excitation monochromator was set at 305 nm and the emission monochromator was set at 390 and 480 nm to detect monomer and excimer emission, respectively. The bandwidth of the excitation and emission monochromators was 16 nm. Ultrahigh-purity hydrogen was used in the flash lamp and gave an average instrument response function of 3.4 ns (fullwidth at half-maximum). Numerical analysis of fluorescence decay data was performed on a DEC PDP-11/44 computer with software developed in our laboratory. The approach uses the method of reiterative convolution with SIMPLEX optimization of the lifetime and amplitude factors to minimize the deviations between the calculated and experimental fluorescence decay profiles.

The approach of "component incrementation", introduced by Isenberg et al., was applied to determine the number of components present in the monomer and excimer decay profiles.<sup>8</sup> In this method, one analyzes the data by using successively higher numbers of components until no significant change occurs in the calculated amplitude factors or lifetimes. For example, if one analyzes for two components and finds that one of them is close to the values obtained in a one-component analysis, while the other has a very low amplitude factor compared with the first, this would imply that a one-component analysis conforms to the data and no attempt should be made to fit the data to more than one component. However, if the two components have amplitude factors of the same order of magnitude with different lifetimes, one would analyze for three components.

This method provides a good means to evaluate the validity of the statistical analysis by which the lifetimes and amplitude factors are adjusted to minimize reduced  $\chi^2$ ; the sum of the statistically weighted squares of the residuals between the calculated and experimental

Table I. Typical Goodness-of-Fit Criteria for Monomer Emission<sup>a</sup>

surf concn, $\mu mol/m^2$	no. of components	amp factor	lifetime, ns	$\chi^2_v$	
0.20	1	1.00	59.0	4.796	
		0.24	9.7	1.193	
	2	0.76	61.3		
		0.21	2.4	1.090	
		0.14	15.1		
	3	0.65	61.8		
		0.19	1.0	1.110	
		0.11	1.9		
		0.14	13.3		
		0.56	61.7		
	0.33	1	1.00	42.2	31.508
			0.63	7.3	2.438
2		0.37	49.6		
		0.54	2.6	1.088	
		0.23	14.8		
3		0.23	52.3		
		0.03	2.6	1.093	
		0.54	2.6		
		0.21	14.7		
		0.22	52.3		

<sup>a</sup> Monomer emission for 3PPS in contact with methanol.

fluorescence decay profiles divided by the number of degrees of freedom.<sup>9</sup> Grinvald and Steinberg pointed out that the variation in the weighted sum of the squares of the residuals due to a change in the value of one parameter can be compensated to a considerable extent by a corresponding change in one or more of the other parameters.<sup>10</sup> Thus,  $\chi^2_v$  is relatively insensitive to concerted changes in the values of the parameters, and this problem becomes more severe as the number of parameters is increased.

In general, we have found that when  $(\chi^2_v)_{min} \geq 1.5$ , the actual decay law is not given by the model which was fitted to the data. On the other hand, for values of  $(\chi^2_v)_{min} < 1.5$ , it was necessary that both statistical ( $\chi^2_v$ ) and experimental (component incrementation) criteria be used in judging the goodness of fit of the model decay law. Table I contains the data for applying these joint criteria and, accepting this analytical approach, it can be seen that a three-component model (eq 1) provides the best statistical and experimental fit of the data over the surface concentrations studied.

$$I_f(t) = A_1 e^{-t/\tau_1} + A_2 e^{-t/\tau_2} + A_3 e^{-t/\tau_3} \quad (1)$$

### Results and Discussion

**3PPS Proximity and Distribution on the Silica Surface.** The physical significance of the amplitude factors ( $A_i$ ) presented in eq 1 is arrived at as follows. Assume that  $N_i$  molecules of the  $i$ th species are excited at zero time and all emission intensity is observed. The quantum yield of the  $i$ th component,  $\Phi_i$ , is represented by<sup>10</sup>

$$\Phi_i = \int_0^\infty \frac{A_i e^{-t/\tau_i} dt}{N_i} = \frac{A_i \tau_i}{N_i} \quad (2)$$

$$A_i = \Phi_i N_i / \tau_i \quad (3)$$

where  $t$  is time,  $\tau_i$  is the radiative lifetime of the  $i$ th component, and  $A_i$  is the amplitude factor of the  $i$ th component. By definition the quantum yield of the  $i$ th component is represented by eq 4 and substitution of eq 3 results in the amplitude factor being equal to the product of the number of molecules and natural radiative lifetime of the  $i$ th component ( $\tau_i^0$ ), eq 5. The amplitude factor

$$\Phi_i = \tau_i / \tau_i^0 \quad (4)$$

$$A_i = N_i / \tau_i^0 \quad (5)$$

is found to be directly proportional to the number of molecules excited at time zero; furthermore, if  $\tau_i^0$  is found to be equal for all values of  $i$  and the fraction of the emission collected and

(3) Burke, M. F.; Yonker, C. R.; Zwier, T. A. *J. Chromatogr.* **1982**, *241*, 257.

(4) Burke, M. F.; Yonker, C. R.; Zwier, T. A. *J. Chromatogr.* **1982**, *241*, 345.

(5) Gilpin, R. K.; Gangoda, M. E.; Krishen, A. E. *J. Chromatogr. Sci.* **1982**, *20*, 345.

(6) McCormick, R. M.; Karger, B. L. *J. Chromatogr.* **1980**, *199*, 259.

(7) Scott, R. P. W.; Simpson, C. F. *Symp. Faraday Soc.* **1980**, *15*, 69.

(8) Isenberg, I.; Dyson, R. D.; Hanson, R. *Biophys. J.* **1973**, *13*, 1090.

(9) Bevington, P. R. "Data Reduction and Error Analysis for the Physical Sciences"; McGraw-Hill: New York, 1969.

(10) Grinvald, A.; Steinberg, I. Z. *Anal. Biochem.* **1974**, *59*, 583.

**Table II.** Normalized Monomer Preexponential Factors ( $A_i$ ) and Lifetimes ( $\tau_i$ ) as a Function of Solvent and Surface Concentration

	surf concn, $\mu\text{mol}/\text{m}^2$					
	0.13	0.20	0.33	0.57	0.70	1.10
Methanol						
$A_1$	0.21	0.25	0.61	0.76	0.82	0.87
$A_2$	0.15	0.16	0.21	0.18	0.14	0.12
$A_3$	0.64	0.59	0.18	0.06	0.04	0.01
$\tau_1$	2.9	2.2	2.2	2.7	1.9	1.4
$\tau_2$	19.2	19.8	14.6	15.6	14.2	5.6
$\tau_3$	66.0	66.6	53.2	65.2	69.8	37.3
Acetonitrile						
$A_1$		0.20	0.63	0.76	0.83	0.92
$A_2$		0.23	0.23	0.20	0.13	0.07
$A_3$		0.57	0.14	0.04	0.04	0.01
$\tau_1$		2.7	2.8	2.1	2.0	1.5
$\tau_2$		15.2	17.5	10.8	12.9	5.6
$\tau_3$		44.9	56.6	49.8	56.2	30.5
Tetrahydrofuran						
$A_1$		0.21	0.53	0.67	0.69	0.75
$A_2$		0.40	0.31	0.27	0.26	0.23
$A_3$		0.39	0.16	0.06	0.05	0.02
$\tau_1$		11.1	5.1	4.8	3.1	3.5
$\tau_2$		39.8	21.8	19.3	14.6	8.1
$\tau_3$		67.4	60.4	69.1	69.0	34.3
Hexane						
$A_1$		0.11	0.43	0.52	0.62	0.67
$A_2$		0.28	0.41	0.41	0.33	0.30
$A_3$		0.61	0.16	0.07	0.05	0.03
$\tau_1$		4.2	2.9	2.9	2.2	2.4
$\tau_2$		10.8	12.8	10.4	8.2	6.4
$\tau_3$		26.8	28.1	28.4	24.6	26.1

detected remains constant, then the *normalized* amplitude factors presented in Table II represent the fraction of the total monomer population that decays with a lifetime  $\tau_i$  for a given value of  $i$ .

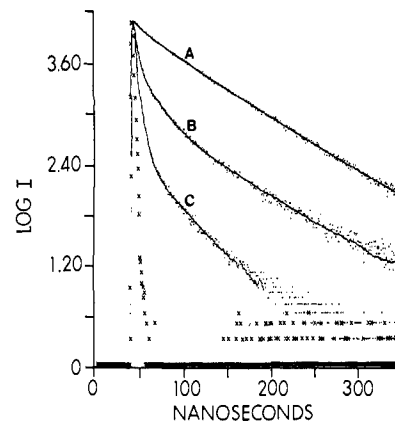
The assumption that  $\tau_i^\circ$  for  $i = 1-3$  are equivalent can be made provided that the molar absorptivity ( $a_i$ ) for each component is equivalent and each component has the same ground- and excited-state potential energy surface. The assumption is very probable in this case since all 3PPS molecules are bound to the surface via the siloxane linkage and any resulting perturbation of electronic structure would be expected to be equivalent for all 3PPS molecules. In the absence of any deactivating perturbation, the molecule's natural radiative lifetime,  $\tau^\circ$ , is inversely related to the integrated absorption intensity as given by eq 6,<sup>11</sup> where  $n$  is the refractive index of the medium,  $\bar{\nu}$  is the wavenumber of absorption, and  $\bar{\nu}_0$  is the wavenumber of the approximate mirror image reflection plane of the absorption and fluorescence spectra.

$$\frac{1}{\tau_i^\circ} = 2.88 \times 10^{-9} n^2 \int \frac{(2\bar{\nu}_0 - \bar{\nu})^3}{\bar{\nu}} a_\nu d\bar{\nu} \quad (6)$$

Equation 6 requires a mirror symmetry relation between the fluorescence and absorption spectra; that is, it depends on the existence of an approximately parallel nature of the potential energy surfaces for the ground and excited states of a molecule where the bond lengths are little affected because of delocalization of electronic energy followed absorption.<sup>12</sup> The monomer excitation and emission spectra previously reported for 3PPS bound to silica indicate that such a relationship exists.<sup>1</sup> Furthermore, the monomer emission and excitation spectra show no wavelength shift with increasing concentration. Thus, all the 3PPS molecules would reside in the same lowest excited singlet state and have a natural radiative lifetime dependent on the transition probability of absorption which is proportional to the integral in eq 6. The *normalized* amplitude factors presented in Table II are therefore a fair estimate of the fraction of the total monomer population

(11) Parker, C. A. "Photoluminescence of Solutions"; Elsevier: New York, 1968.

(12) Rohatgi-Mukherjee, K. K. "Fundamentals of Photochemistry"; Wiley: New York, 1978.

**Figure 1.** Monomer decay curves for 3PPS bonded on Partisil 10: solvent methanol,  $A = 0.13 \mu\text{mol}/\text{m}^2$ ,  $B = 0.57 \mu\text{mol}/\text{m}^2$ ,  $C = 1.10 \mu\text{mol}/\text{m}^2$ .**Table III.** Excimer Rise Times as a Function of Solvent and Surface Concentration<sup>a</sup>

surf concn, $\mu\text{mol}/\text{m}^2$	methanol	acetonitrile	tetrahydrofuran	hexane
0.13	4.9			
0.20	4.2	2.9	9.1	5.6
0.33	3.6	2.4	5.6	4.8
0.57	2.3	1.7	4.6	3.4
0.70	1.4	1.4	3.6	2.8
1.10	1.2	1.3	3.5	2.3

<sup>a</sup>Rise times reported in nanoseconds.

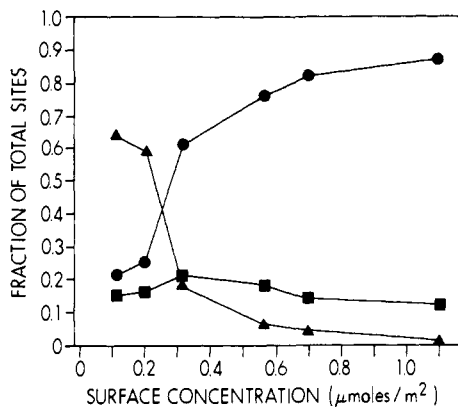
excited at  $t = 0$  with an average lifetime ( $\tau_i$ ) for a given value of  $i$ .

Figure 1 presents typical monomer decay profiles obtained in methanol for three different surface concentrations of 3PPS. The amplitude factors and lifetimes for the monomer decay curves obtained for all solvents studied are contained in Table II. These results indicate deviations from the conventional, diffusion-controlled model developed by Birks to describe the intermolecular excimer kinetics for small aromatic compounds in liquid solution.<sup>13</sup> In fact, the results obtained more closely resemble those observed for intramolecular excimer formation, which is not diffusion controlled. Departures from true, diffusion-controlled behavior might be expected in constrained systems where the chromophores either are linked by short alkyl chains or are chemically bound in close proximity on a silica surface.

Close examination of the amplitude factors and lifetimes in Table II reveals what appears to be three distinct monomer populations. The lifetimes  $\tau_1$ ,  $\tau_2$ , and  $\tau_3$  each remain relatively constant for a particular solvent over the surface concentrations studied except at near-saturation coverage ( $1.10 \mu\text{mol}/\text{m}^2$ ). The consistency of these lifetimes for a particular solvent suggests that there are three major distinct populations of 3PPS molecules bound to the surface which fluoresce with characteristic rate constants that are independent of each other. The decrease in lifetimes at  $1.10 \mu\text{mol}/\text{m}^2$  is believed to be due to increased collisional quenching resulting from the densely packed surface obtained at near-saturation coverage.

The  $A_2$  population appears to represent an "isolated" fraction of the monomer population incapable of excimer formation because the distance between adjacent 3PPS bonding sites is too great. The absence of a rise time component (Table III) in the excimer decay profile corresponding to the monomer lifetime ( $\tau_2$ ) implies that the growth of the excimer emission does not occur at the expense of the  $A_2$  monomer population. Furthermore, the fraction of molecules in the  $A_2$  population remains relatively constant over the surface concentrations studied for each solvent and is consistent with the idea of a truly "isolated" population of bound molecules. The  $A_1$  and  $A_3$  amplitude factors exhibit a monotonic increase and decrease, respectively (Figure 2), with increasing surface

(13) Birks, J. B. *Rep. Prog. Phys.* **1975**, *38*, 903.



**Figure 2.** Monomer population distribution as a function of surface concentration: solvent methanol, (●)  $A_1$ , (■)  $A_2$ , (▲)  $A_3$ .

concentration, and are apparently related since the  $A_3$  population disappears with the same concentration dependence as the growth of the  $A_1$  population. This reduction of the relative  $A_3$  population by "excimer-forming" monomers reflects the fraction of bonded 3PPS ligands (excluding the  $A_2$  monomer population) that become clustered with increasing surface concentration. It should be emphasized that the number of molecules associated with the "non-excimer-forming"  $A_3$  population does not decrease due to quenching by the  $A_1$  population, but rather it is the fraction of  $A_3$  molecules relative to the total population that decreases with increasing surface concentration. The constancy of the  $\tau_1$  and  $\tau_3$  lifetimes is in agreement with this observation since  $\tau_3$  would be expected to decrease if the growth of the  $A_1$  population was due to quenching of the  $A_3$  population with increasing surface concentration. The excimer rise times presented in Table III agree well with the lifetimes of the  $A_1$  monomer component, and this in addition to the growth in  $A_1$  with increased excimer emission (obtained from steady-state measurements)<sup>1</sup> confirms that the  $A_1$  monomer population is responsible for excimer emission. Finally, the possibility of monomer emission resulting from excimer dissociation can be assumed to be negligible since there is no apparent rise time associated with the monomer decay profiles.

Precise, space-filling models of 3PPS were constructed to estimate the maximum distance between 3PPS bonding sites that would permit excimer formation assuming a fixed critical interaction distance of 4.0 Å with maximum overlap of the pyrene rings and free rotation about the siloxane bond between the organosilane and the silica surface. Figure 3 presents structural conformations and the corresponding maximum distance between 3PPS bonding sites for the fully extended, collapsed, and "pore" or interparticle representations for 3PPS molecules bound to the silica substrate. Interparticle or "pore" excimer formation can be assumed to be negligible as the mean pore diameter of Partisil 10 is approximately 4 times greater than the maximum distance between bonding sites. The maximum possible distance between bonding sites for excimer formation occurs in the collapsed state of Figure 3B. Molecules with greater than 18.4-Å separation form the "isolated" monomer population,  $A_2$ .

The  $(N)_{\text{excimer}}/(N)_{\text{monomer}}$  ratio is plotted in Figure 4 against surface concentration and the average distance between homogeneously distributed bonding sites. The sum of the  $A_2$  and  $A_3$  factors is that fraction of the total 3PPS population which is "isolated" and cannot form excimers,  $(N)_{\text{monomer}}$ . The  $A_1$  factor is related to the "excimer-forming" monomer population and is therefore equivalent to the number of 3PPS molecules that emit as excimers,  $(N)_{\text{excimer}}$ . Figure 4 suggests that 50% of the bound molecules in contact with methanol occur within the interaction distance for excimer formation at  $D_{\text{expt}}$  equal to 25.6 Å. No excimer formation would be expected at this distance unless the distribution of chemically reactive silanols is not homogeneous and that covalently bound pyrene molecules occur in clusters.

The results for 3PPS silica in contact with methanol might suggest that the extent of clustering is solely determined by the distribution of chemically reactive silanols; however, significant

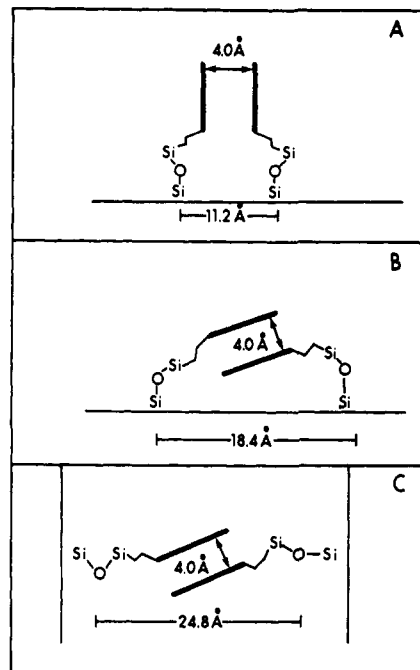


**Figure 3.** Structural conformations for 3PPS bonded on Partisil 10: Figure represents hypothetical structural types, not specific structural arrangements. A = fully extended, B = collapsed, C = pore or interparticle 3PPS conformation.

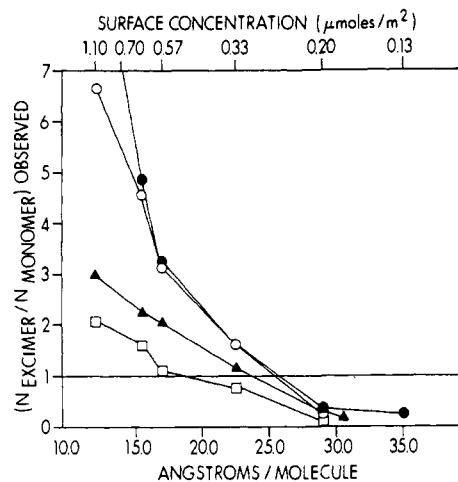


**Figure 4.** Observed excimer/monomer population ratio as a function of surface concentration and average distance between bonding sites for different solvents: (●) acetonitrile, (○) methanol, (▲) tetrahydrofuran, (□) hexane.

differences in the values of  $D_{\text{expt}}$  at an  $(N)_{\text{excimer}}/(N)_{\text{monomer}}$  ratio equal to 1.0 are observed for different solvents. These observed differences must be due to variations in solvation which result in preferred, solvent-induced conformations of the bound molecules. The  $D_{\text{expt}}$  values for methanol, acetonitrile, and tetrahydrofuran at  $(N)_{\text{excimer}}/(N)_{\text{monomer}}$  equal to 1.0 are all greater than that needed for excimer formation. A fully extended conformation is most likely in hexane and the  $D_{\text{expt}}$  value observed for hexane confirms this. At near-saturation coverage, the factors  $A_1$ ,  $A_2$ , and  $A_3$  allow for a quantitative estimate of the proximity and distribution of bound molecules. It appears that the three populations are those having nearest neighbors at distances greater than 18.4 Å (10%), between 18.4 and 11.2 Å (20%) and less than 11.2 Å (70%). The variation in these populations with solvent are apparent in Figure 5 and are discussed in the following section.

**Solvent-Induced Conformation Changes of Bound 3PPS Molecules.** The results discussed in the previous section indicate that although the proximity and distribution of chemically reactive silanols dominates the organization of bound molecules on silica,

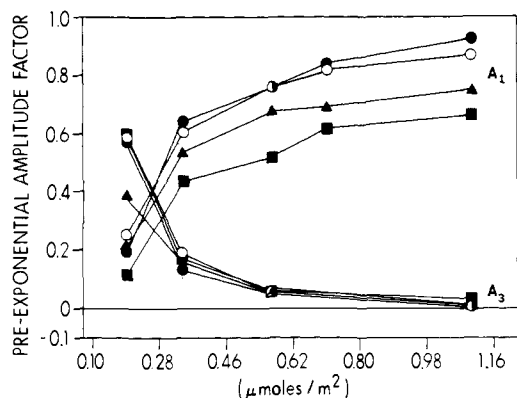


Figure 5. Variation of 3PPS monomer populations as a function of solvent and surface concentration: (●) acetonitrile, (▲) tetrahydrofuran, (■) hexane, (○) methanol.

differences in solvation of the bound ligands can account for approximately a 20% change in the distribution of molecular conformations. The variation of the amplitude factors in different solvents can be explained by solvent-induced conformation changes in the bonded phase mass due to "solvophobic" interactions between the bonded ligands and solvent.<sup>14</sup> Solvation of the pyrene moiety results in extension of the bonded ligand as in Figure 3A, but solvents that are more hostile tend to promote collapse of the bonded ligands upon each other and toward the underlying surface as in Figure 3B. The reduction of the total exposed surface area may be the driving force for collapse of the bonded ligands in hostile solvents such as methanol and acetonitrile. Chromatographic and spectroscopic evidence supports solvophobic aggregation of hydrophobic molecules in solvents such as methanol, ethanol, acetonitrile, and water.<sup>15-19</sup> The picture that emerges for 3PPS molecules bound to the surface is that of a "breathing" surface, is suggested by Martire and Boehm,<sup>20</sup> where the bonded ligands attempt to adjust their total surface area exposed to solvent depending on the solvating properties of the solvent.

The  $A_1$  and  $A_3$  amplitude factors are plotted in Figure 5 as a function of surface coverage for 3PPS silicas in contact with different solvents. The  $A_3$  factors show nearly identical behavior for all surface concentrations irrespective of solvent and represent the fraction of "potential excimer" bonding sites. The normalized  $A_1$  factors at near-saturation coverage ( $1.1 \mu\text{mol}/\text{m}^2$ ) for acetonitrile and methanol indicate that approximately 90% of adjacent 3PPS bonding sites must be within  $18.4 \text{ \AA}$ . The  $A_1$  values for tetrahydrofuran and hexane at  $1.1 \mu\text{mol}/\text{m}^2$  indicate that actually 70% of the 3PPS bonding sites are within  $11.2 \text{ \AA}$  and that the observed differences in  $A_1$  reflect the alteration of the bonded-phase conformation. The average  $A_2$  values are observed to increase from methanol (0.16) to hexane (0.34) as would be expected for an increased population of "isolated monomers".

These changes in bonded-phase conformation due to enhanced solvation are further supported by the excimer rise times. The rise times for excimer formation of the 3PPS silicas reflect the time required for reorientation of the bonded ligands into the preferred conformation for excimer formation. Solvent-induced conformation changes that affect the relative mobility of bound ligands should be reflected in the rise time data. Figure 6 shows the excimer decay profile for bound 3PPS in methanol. The excimer decay profiles are the sum of three exponentials. Table III presents the rise times obtained in the different solvents as a function of surface concentration and show that the rise times for tetrahydrofuran and hexane are appreciably longer than those

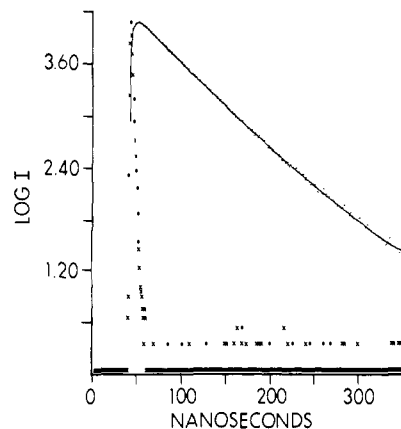


Figure 6. Excimer decay curve for 3PPPs bonded on Partisil 10: solvent methanol,  $0.13 \mu\text{mol}/\text{m}^2$ .

for methanol and acetonitrile at all surface concentrations studied. These differences in rise time reflect the changes in mobility of the bound 3PPS ligands. Although the differences are small, they are well within the time resolution of the instrument and differ significantly from excimer rise times reported for intramolecular excimer formation and pyrene adsorbed on silica gel.<sup>17,21,22</sup>

Ghiggino et al.<sup>17</sup> have reported on the kinetics of intramolecular excimer formation of dipyrenylalkanes. Their studies indicate that solvent interactions with the chains linking chromophores can alter both their flexibility and extension and that the observed differences in excimer formation kinetics are due to differing degrees of solvent influence on the rigidity of the connecting hydrocarbon chain. This evidence strongly supports the suggestion that the rise times presented in Table III are consistent with the model of solvent-induced conformation changes of the bonded phase due to solvophobic interactions.

Recent investigations by Ware et al.<sup>21,22</sup> reporting the photophysics of pyrene adsorbed on porous silica have shown that pyrene excimer emission exhibits a rise time characteristic of dynamic excimer formation only in the presence of coadsorbed molecules such as long-chain alcohols. The results reported here and those previously presented<sup>1</sup> indicate that excimer emission from 3PPS-derivatized silica in contact with solvent is due to the formation of an excited-state dimer (excimer) rather than by the excitation of a ground-state dimer as suggested in that work. The excimer decay curves presented by Ware et al. representing static quenching of the dynamic excimer formation by bimolecular ground-state associations are qualitatively very similar to the excimer decay curves obtained with the 3PPS silicas at near-saturation coverage. Unfortunately, no quantitative comparison of the excimer decay curves can be made since no time-dependent data for excimer emission were reported.

The observed similarity of the excimer decay curves at saturation coverage with the "excimer-like" decay curves observed by Ware et al.<sup>21,22</sup> is significant because of the proximity and distribution requirements necessary for bound 3PPS molecules to approach the bimolecular ground-state case where the excimer rise times may be assumed to be instantaneous. The possibility exists that the pyrene rings of the 3PPS molecule undergo "cooperative sorption" with each other to minimize their exposed surface area to hostile solvents. The observation that the rise times for tetrahydrofuran and methanol are not constant and differ by more than 2 ns for surface concentrations greater than or equal to  $0.33 \mu\text{mol}/\text{m}^2$  indicates that the proximity and distribution of the bound 3PPS molecules rather than "cooperative sorption" accounts for the short excimer rise times.

The rise time data in Table III show an apparent anomaly with the monomer  $A_1$  amplitude factors for tetrahydrofuran and hexane.

(14) Horvath, C.; Melander, W. *J. Chromatogr. Sci.* **1977**, *15*, 393.

(15) Nakajima, A. *J. Lumin.* **1977**, *15*, 277.

(16) Johnson, G. D. *J. Chem. Phys.* **1975**, *63*, 4047.

(17) Ghiggino, K. P.; Snare, M. J.; Thistlethwaite, P. J. *J. Am. Chem. Soc.* **1983**, *105*, 3328.

(18) Gilpin, R. K. *Am. Lab. (Boston)* **1982**, *14*, 104.

(19) Lochmüller, C. H.; Wilder, D. R. *J. Chromatogr. Sci.* **1979**, *17*, 574.

(20) Martire, D. E.; Boehm, R. E. *J. Phys. Chem.* **1983**, *87*, 1045.

(21) Ware, W. R.; Bauer, R. K.; de Mayo, P.; Wu, K. C. *J. Phys. Chem.* **1982**, *86*, 3781.

(22) Ware, W. R.; Bauer, R. K.; de Mayo, P.; Okada, K.; Wu, K. C. *J. Phys. Chem.* **1982**, *87*, 460.

The rise times for excimer formation in hexane are expected to be longer than those obtained in tetrahydrofuran due to enhanced solvation of the 3PPS ligands in hexane as reflected by the  $A_1$  and  $A_2$  amplitude factors. In better solvents it is expected that during the conformational rearrangement required for excimer formation there is an enhanced tendency for solvent-3PPS interactions resulting in an increased effective van der Waals volume of the interacting groups and an increased rise time.<sup>16</sup>

The observed deviation may be explained in terms of the structure of the solvent shell surrounding the bound 3PPS ligands and the regiosolvation of the hydrated silica surface. The hydrated silica surface has been proposed to consist of multilayers of adsorbed water. This concept of multilayer adsorption of water on porous silica surfaces is not novel and has been proposed by other investigators.<sup>23-25</sup> Scott and Kucera observed that Langmuir-type, monolayer adsorption isotherms appeared to apply only to the sorption of nonpolar solvents and were inadequate to describe the adsorption isotherms of polar solvents or solvents that could form hydrogen bonds.<sup>26,27</sup> It was found that for nonpolar, non-hydrogen-bonding solvents a monolayer of solvent was adsorbed on the hydrated surface and that polar, hydrogen-bonding solvents were able to displace the weakly adsorbed water layers and to interact directly with the strongly hydrogen-bound, hydrated silanol groups.

Polar, hydrogen-bonding solvents such as tetrahydrofuran and methanol would be expected to extensively solvate the hydrated silica surface by displacing the weakly adsorbed layers of water and interacting directly with the strongly hydrogen bound water layer. Acetonitrile would not be predicted to solvate the hydrated silica surface to the same extent since it is unable to form hydrogen bonds to effectively displace both layers of weakly adsorbed water, and hexane would be expected to form an adsorbed monolayer on the hydrated surface with minimal displacement of the adsorbed water layers. The limited solubility of 3PPS in methanol and acetonitrile could induce solvophobic aggregation of the bonded ligands and thus be predicted to produce the shortest rise times since the ligands would be trapped in a collapsed and highly constrained state with limited rotational or translational motion. The rise times in Table III are consistent with this interpretation and could possibly indicate that at lower surface coverages the longer rise times obtained in methanol reflect the ability of methanol to more effectively solvate and displace the adsorbed

water layers than acetonitrile. The 3PPS ligands would therefore be expected to have greater flexibility in the methanol solvent matrix since much more of the structured water multilayer that could restrict the motion of the bound pyrene molecules due to solvophobic interactions would be displaced relative to the acetonitrile solvent matrix. This same concept of solvation of the structured water multilayer can be applied to explain the observed differences in rise times for the fully extended 3PPS conformers obtained in hexane and tetrahydrofuran.

The long-lived monomer lifetimes  $\tau_3$  support the idea that the more polar, hydrogen-bonding solvents more effectively disrupt the structured water multilayer by displacing all water layers excluding the strongly adsorbed layer that is hydrogen bonded directly to the surface silanols. Longer lifetimes are observed in Table II for tetrahydrofuran and methanol where water is not able to effectively quench the long-lived monomer lifetime  $\tau_3$  as in the case of acetonitrile or the worst case, hexane. The dramatic decrease in the  $\tau_3$  lifetimes at saturation coverage ( $1.1 \mu\text{mol}/\text{m}^2$ ) is indicative of concentration quenching of the long-lived monomer component as the 3PPS molecules become more densely packed on the silica surface and is supported by the decay of the  $A_3$  monomer amplitude factors and the gradual decrease in excimer rise times as a function of surface concentration.

### Conclusions

The results indicate that the proximity and distribution of chemically reactive silanols primarily determine the organization of bound molecules and that solvent-induced conformation changes result in approximately a 20% change in the organization of bound molecules on the silica surface. A quantitative estimate of the proximity and distribution of bound molecules from the results obtained suggests that there are three populations having nearest neighbors at distances greater than  $18.4 \text{ \AA}$  (10%), between  $18.4$  and  $11.2 \text{ \AA}$  (20%), and less than  $11.2 \text{ \AA}$  (70%). The picture that emerges is an inhomogeneous distribution of chemically bonded molecules where "clustering" predominates and where the solvent properties of the mobile phase modify the organization of bound molecules on the silica surface.

**Acknowledgment.** This work was supported, in part, by a grant from the National Science Foundation (Grant CHE-8119600 to C.H.L.). J.M.H. acknowledges the donors of the Petroleum Research Fund, administered by the American Chemical Society, for partial support of this research. The silica was drawn from the Duke Standard Substrate Collection established by a gift from Whatman-Chemical Separations. Aliquots of these materials are available to serious investigators upon request.

Registry No. 3PPS, 86278-57-1.

(23) Scott, R. P. W.; Traiman, S. *J. Chromatogr.* **1980**, *196*, 193.

(24) Mitchell, S. A. *Chem. Ind. (London)* **1966**, 924.

(25) Linsen, B. G., Ed. "The Physical and Chemical Aspects of Adsorbents and Catalyst"; Academic Press: New York, 1970.

(26) Scott, R. P. W.; Kucera, P. *J. Chromatogr.* **1978**, *149*, 93.

(27) Scott, R. P. W.; Kucera, P. *J. Chromatogr.* **1979**, *171*, 37.